Enriched Protein Screening of Human Bone Marrow Mesenchymal Stromal Cell Secretions Reveals MFAP5 and PENK as Novel IL-10 Modulators

Jack M Milwid[1,2], Jessica S Elman[1], Matthew Li[1–3], Keyue Shen[1], Arjun Manrai[2], Aaron Gabow[4], Joshua Yarmush[6], Yunxin Jiao[1], Anne Fletcher[5], Jungwoo Lee[1], Michael J Cima[3], Martin L Yarmush[1,6] and Biju Parekkadan[1,7]

[1]Department of Surgery, Center for Engineering in Medicine and Surgical Services, Massachusetts General Hospital, Harvard Medical School, Boston, Massachusetts, USA; [2]Harvard-MIT Division of Health Sciences and Technology, Massachusetts Institute of Technology, Cambridge, Massachusetts, USA; [3]David H. Koch Institute for Integrative Cancer Research, Massachusetts Institute of Technology, Cambridge, Massachusetts, USA; [4]Computational Biology Center, Memorial Sloan-Kettering Cancer Center, New York, New York, USA; [5]Dana-Farber Cancer Institute, Harvard Medical School, Boston, Massachusetts, USA; [6]Department of Biomedical Engineering, Rutgers University, Piscataway, New Jersey, USA; [7]Harvard Stem Cell Institute, Cambridge, Massachusetts, USA

The secreted proteins from a cell constitute a natural biologic library that can offer significant insight into human health and disease. Discovering new secreted proteins from cells is bounded by the limitations of traditional separation and detection tools to physically fractionate and analyze samples. Here, we present a new method to systematically identify bioactive cell-secreted proteins that circumvent traditional proteomic methods by first enriching for protein candidates by differential gene expression profiling. The bone marrow stromal cell secretome was analyzed using enriched gene expression datasets in combination with potency assay testing. Four proteins expressed by stromal cells with previously unknown anti-inflammatory properties were identified, two of which provided a significant survival benefit to mice challenged with lethal endotoxic shock. Greater than 85% of secreted factors were recaptured that were otherwise undetected by proteomic methods, and remarkable hit rates of 18% *in vitro* and 9% *in vivo* were achieved.

Received 15 July 2013; accepted 30 January 2014; advance online publication 18 March 2014. doi:10.1038/mt.2014.17

INTRODUCTION

Cells can communicate by secreting proteins that act on neighboring or distant target cells to regulate function and phenotype. Identification of these communication signals has led to a deeper understanding of physiological processes involved in health and disease, including cell proliferation,[1] differentiation,[2] motility,[3] and apoptosis.[4] Secreted proteins have also become important in the development of some of the most successful therapies in history. These therapies are generally designed to either increase the natural levels by administration of recombinant proteins or decreasing the level by use of neutralizing agents, such as antibodies. Insulin, a secreted pancreatic hormone, has been supplemented for decades as a first-line therapy for regulating the uptake of glucose by target cells in diabetic patients (2011 US sales: $9.8B).[5,6] Interferon-α and interferon-β are widely used to treat hepatitis C virus infection and multiple sclerosis, respectively (collective 2011 US sales: $2.5B).[6,7] Proinflammatory cytokines, such as tumor necrosis factor (TNF)-α, have become mega-blockbuster pharmaceutical targets for patients with autoimmune diseases (2011 US sales of TNF-α inhibitors: $6.8B).[6,8] Total US sales in 2011 of protein drugs based on native secreted proteins exceeded $32B.[6]

Identification of secreted proteins has primarily relied on hypothesis-driven interrogation and is limited to known biological pathways.[9] Open-ended screening approaches that assume less about the underlying biology are impractical because establishment of libraries of all known secreted proteins is cost-prohibitive; probing the vast interactome is intractable; and not all proteins synthesized in the human body can be made recombinantly.[10] A bottom-up approach to access and dissect a finite library of secreted proteins involves the analysis of conditioned medium (CM) from a cell. Traditional biochemical methods for characterizing CM, such as liquid chromatography (LC) and mass spectrometry (MS), have led to the discovery of many important proteins including interferon and hepatocyte growth factor.[11,12] These methods are, however, labor intensive because of the need to grow billions of cells in order to generate liters of CM and eliminate serum and albumin contaminants for sensitive analysis.[13,14] These challenges have restricted discovery efforts in academic and industrial laboratories. New methods to elucidate secreted proteins and the pathways they influence can accelerate the discovery of new signaling molecules for biological research and therapeutic testing.

A new, simple method for discovering potential secreted protein communication pathways is reported here. The method

Correspondence: Biju Parekkadan, Department of Surgery, Center for Engineering in Medicine and Surgical Services, Massachusetts General Hospital, Harvard Medical School, Boston, Massachusetts 02114, USA. E-mail: biju_parekkadan@hms.harvard.edu

(referred to as enriched protein screening (EPS)) circumvents the need for LC/MS by using comparative gene profiling to enrich for active secreted proteins that can be recombinantly screened in bioassays (**Figure 1**). A human peripheral blood mononuclear cell (PBMC) inflammation assay was used to screen candidates naturally expressed by human bone marrow mesenchymal stromal cells (BM-MSCs)[15] as a proof of concept. BM-MSCs are stem-like cells that are being explored clinically as a therapeutic for a variety of inflammatory and autoimmune diseases.[16] The implementation of EPS led to the discovery of two novel immunomodulatory proteins, microfibrillar-associated protein 5 (MFAP5) and unprocessed proenkephalin (PENK), that when administered to mice subjected to endotoxemic shock, reversed the cytokine storm and provided a significant survival benefit comparable to the gold-standard anti-inflammatory biologic, monoclonal anti-TNF-α antibodies.

RESULTS

Development of a human blood potency assay to analyze BM-MSC–secreted factors

BM-MSCs have been extensively reported to have anti-inflammatory properties when used in a transplantation setting.[17] Interleukin (IL)-10 is increased in the serum of inflamed rodents after treatment with BM-MSCs or a bolus of concentrated BM-MSC-CM.[18] A potency assay was developed to recapitulate this IL-10 response *in vitro* using primary human PBMCs to evaluate the bulk anti-inflammatory activity of BM-MSC-CM (**Figure 2a**). PBMCs were incubated with BM-MSC-CM and then stimulated with lipopolysaccharide (LPS) to instigate a proinflammatory response. LPS-stimulated production of IL-10 by human PBMCs increased significantly when the cells were preincubated with BM-MSC-CM (**Figure 2b**; **Supplementary Figure S2a**). Upregulation of IL-10 release was dose dependent (**Figure 2c**), suggesting that the receptors responsible for IL-10 release were not saturated in this range of CM. Digestion of BM-MSC-CM with proteinase K attenuated the IL-10 response, confirming the causative role of proteins in the CM (**Supplementary Figure S2b**). BM-MSC-CM also suppressed inflammatory interferon (IFN)-γ production in this assay (**Supplementary Figure S3**). Boosting of IL-10 was further used as an assay endpoint because it is less prone to nonspecific assay artifacts, such as suppressed IFN-γ expression from cytotoxicity. The sensitivity of the PBMC assay was tested using fractions of BM-MSC-CM based on size (**Supplementary Figure S4a**) and charge (**Supplementary Figure S4b**), and clear delineation of active regions confirmed sufficient detection sensitivity of the assay.

Genomic enrichment of BM-MSC–secreted proteins based on potency

A comparative gene expression scheme was developed to rationally enrich candidate proteins that contribute to the anti-inflammatory

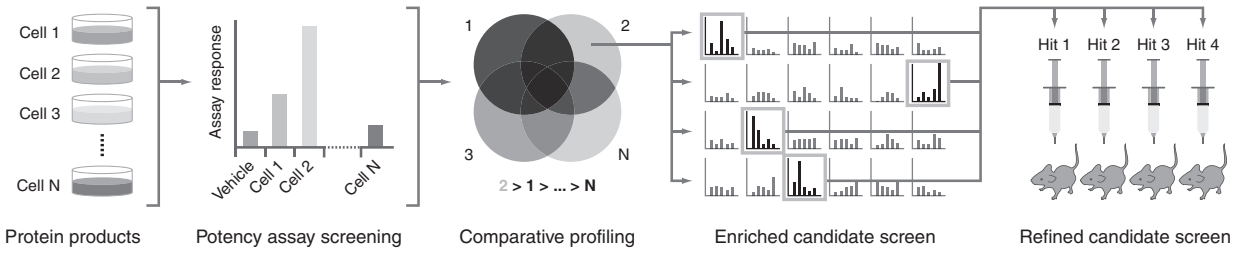

Figure 1 Enriched protein screening (EPS). A generalized schematic of EPS methodology. Protein products are derived from various cell types in the form of conditioned media and screened for activity in an *in vitro* potency assay. Based on the activity of the conditioned media from the cells, differential gene expression profiling is performed to select for genes uniquely upregulated in the cell type with the highest activity in the potency assay. Recombinant protein products of the enriched gene list are then screened in the same potency assay and candidates with the highest activity are assessed for activity *in vivo*.

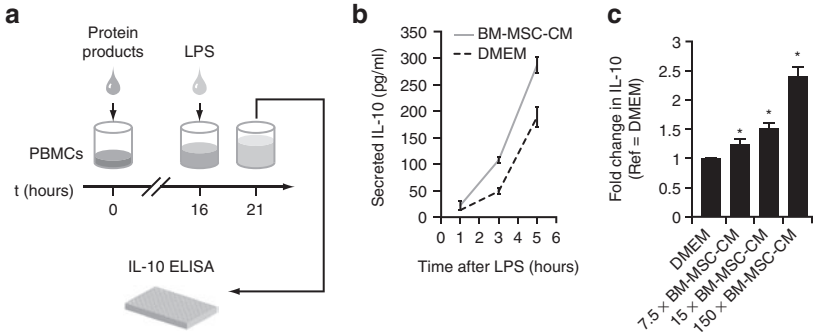

Figure 2 *In vitro* blood inflammation assay. (**a**) An IL-10 *in vitro* potency assay for this study. This assay entails incubating primary human PBMCs in the presence of protein products (*e.g.*, conditioned medium from a cell) for 16 hours, followed by stimulation of the PBMCs with (LPS) for 5 hours, and measurement of IL-10 secretion into the supernatant via ELISA. (**b**) Time course of IL-10 expression from PBMCs when incubated with either bone marrow stromal cell conditioned medium (BM-MSC-CM) or unconditioned medium (DMEM) in the potency assay. (**c**) Dose response of the potency assay to increasing concentration of BM-MSC-CM. 15× CM was either diluted or concentrated further to generate the different concentrations. *N* = 3 independent trials. **P* < 0.001 compared to DMEM. BM-MSC, bone marrow mesenchymal stromal cell; CM: conditioned medium; DMEM, Dulbecco's modified Eagle's medium; LPS, lipopolysaccharide; PBMC, peripheral blood mononuclear cells.

activity of BM-MSC-CM. Genome-wide datasets were established based on the differential potency of CM from three different cell populations in boosting IL-10. BM-MSCs were compared to human skin fibroblasts (FBs), as FBs express many similar genes as BM-MSCs but lacked activity in the PBMC potency assay (**Figure 3a**). Comparison of gene expression of BM-MSCs and FBs, yielded a list of ~500 genes uniquely upregulated in BM-MSCs. Many of the genes that were upregulated in BM-MSCs clustered around an undifferentiated progenitor phenotype and were associated with developmental processes (**Figure 3b**). The second largest enriched cluster was secreted glycoproteins.

An additional genomic dataset from a third cell population was introduced to further refine gene enrichment. This third cell population was an activated BM-MSC to induce a state of heightened potency. BM-MSCs display a number of surface cytokine and toll-like receptors that have been implicated in their immunomodulatory phenotype.[19] BM-MSCs were prestimulated with a selection of proinflammatory ligands prior to conditioning. LPS prestimulation was found to increase the potency of BM-MSC-CM significantly (**Figure 3c**,**d**). Cluster analysis of the BM-MSC$_{LPS}$≥BM-MSC gene set revealed that many of the upregulated genes were associated with an immune response. The next largest cluster in this gene set was secreted glycoproteins, which were preferentially enriched after LPS stimulation (**Figure 3e**). These data further supported the hypothesis that a contrast hierarchy of BM-MSC$_{LPS}$≥BM-MSC>FB would accentuate key secreted molecules responsible for the IL-10 phenomenon. This contrast hierarchy revealed 139 genes (**Figure 3f**). A literature search to determine which of these genes correspond to a secreted protein yielded a highly enriched set of 22 genes (**Figure 3g**).

Recombinant protein library construction and screening

The gene expression hierarchy revealed a highly enriched set of 22 genes that hypothetically encode the secreted proteins that contribute to the IL-10 boosting capacity of BM-MSC-CM. This hypothesis was tested by assembling a purified recombinant protein library based on the 22 candidate genes and screening the proteins in the inflammation assay. The screen was performed using a range of physiologically relevant concentrations and 4 of the 22 screened proteins successfully upregulated IL-10 secretion when present at ~100 nmol/l concentrations,

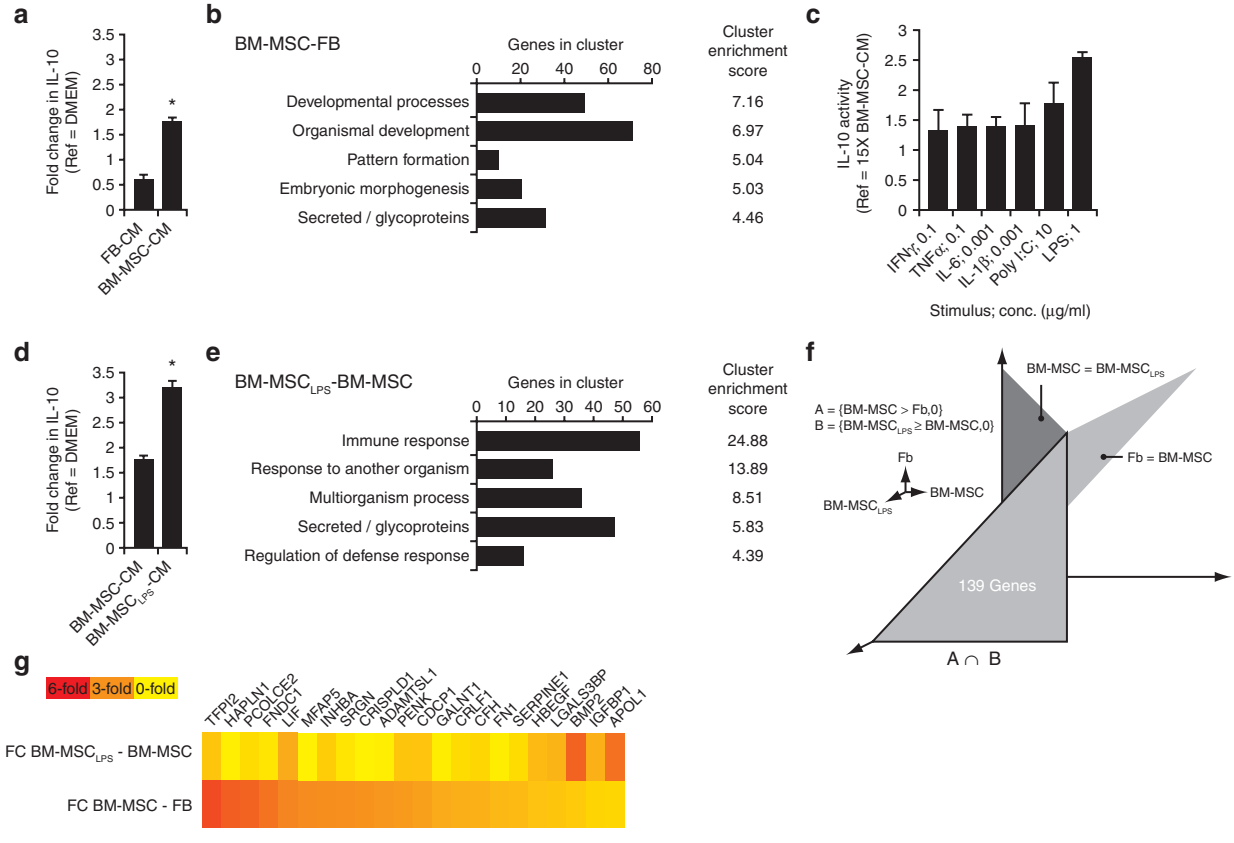

Figure 3 Gene contrast hierarchy and generation of screening library. (**a**) Comparison of potency assay activity of conditioned medium from FB-CM and BM-MSC-CM. *P < 0.001 compared to FB-CM. N = 3 independent trials. (**b**) The top five ontological gene clusters for the contrast set of BM-MSC>FB. N = 3 independent microarrays per group. (**c**) Effect of preconditioning BM-MSCs with stimulatory ligands on the activity of BM-MSC-CM in the potency assay. N = 2 independent trials. (**d**) Comparison of potency assay activity of conditioned medium from BM-MSC-CM and BM-MSCs preincubated with LPS prior to conditioning (BM-MSC$_{LPS}$-CM). *P < 0.001 compared to BM-MSC-CM. N = 3 independent trials. (**e**) Top five ontological gene clusters for the contrast set of BM-MSC$_{LPS}$≥BM-MSC. N = 3 independent microarrays per group. (**f**) Schematic of the gene expression comparison scheme. Genes correlating with anti-inflammatory activity were selected by taking the intersection of the sets of all genes upregulated in BM-MSCs compared to FBs and all genes expressed equally or upregulated in BM-MSC$_{LPS}$ compared to BM-MSCs. (**g**) Gene expression profiling revealed 22 genes responsible for secreted proteins that were upregulated by BM-MSCs stimulated with LPS compared to BM-MSCs and FBs. BM-MSC: bone marrow mesenchymal stromal cell; FB, normal human dermal fibroblasts; LPS: lipopolysaccharide.

polypeptide N-acetylgalactosaminyltransferase 1 (GALNT1), galectin-3-binding protein (LGALS3BP), MFAP5, and PENK (**Figure 4**). Semiquantitative western blots were performed for GALNT1, MFAP5, and PENK, and a quantitative enzyme-linked immunosorbent assay (ELISA) was used for LGALS3BP (**Figure 5a**) to test whether these proteins were present in the BM-MSC-CM. Clear bands were observed for MFAP5 and ELISA results showed LGALS3BP to be present at ng/ml concentrations in the BM-MSC-CM. GALNT1 and PENK were not present at detectable levels, even when the CM was concentrated 100-fold. Proteomic LC/MS was also performed on bulk BM-MSC-CM and several of the 22 proteins in the enriched library were identified, including LGALS3BP (**Figure 5b**). Nevertheless, LC/MS failed to discern 19 of the 22 library proteins (86%) as uniquely expressed by BM-MSCs, including all hits from the PBMC assay screen. Interestingly, no molecules previously reported to be important for BM-MSC therapy were discovered during the EPS analysis. A retrospective gene expression survey revealed that the design of the contrast hierarchy excluded all proteins previously reported to be therapeutic (**Figure 5c**). Certain genes were preferentially upregulated in one of the direct contrast sets but not both, including TGF-β2 in the BM-MSC>FB set and COX-2, IDO, IL-1RAG, IL-6, and TSG-6 in the BM-MSC$_{LPS}$≥BM-MSC set (LogFC>1.5; $P < 0.01$). Taken together, these results demonstrate an unprecedented *in vitro* hit rate of novel protein discovery via EPS (18%), which is several orders of magnitude higher than traditional high throughput approaches for new chemical entities that achieve *in vitro* rates on the order of 0.03–0.2%.[20,21]

In vivo validation of protein candidates

The four hits from the enriched recombinant protein screen were tested for activity *in vivo* in animals challenged with a sub-lethal dose of LPS. Significantly elevated serum IL-10 levels were observed in LPS-treated mice receiving BM-MSC-CM, GALNT1, MFAP5, and PENK compared to baseline vehicle control (saline), but no IL-10 response from LGALS3BP (**Figure 6a**). Serum TNF-α was also significantly suppressed in mice receiving BM-MSC-CM, LGALS3BP, MFAP5, and PENK, but not GALNT1 (**Figure 6a**). In addition, MFAP5 and PENK demonstrated superior TNF-α suppression compared to BM-MSC-CM.

The effects of cytokine modulation were apparent in the lung histology of the animals (**Figure 6b**). In vehicle treated animals, inflammatory infiltrate and alveolar collapse were evident in all lung fields confirming acute lung injury and respiratory distress in this model. LGALS3BP, PENK, and MFAP5 showed increased alveolar space in the majority of the lungs, with slight decreased space in BMSC-CM- and GALNT1-treated mice. PENK, MFAP-5, and BM-MSC-CM showed reductions in apparent inflammatory infiltrate, while GALNT1 and LGALS3BP mice had increased infiltrates. Collectively, only MFAP-5 and PENK had both associated lung changes of increased alveolar space and reduced infiltration that would suggest an overall improvement and protection of LPS injury.

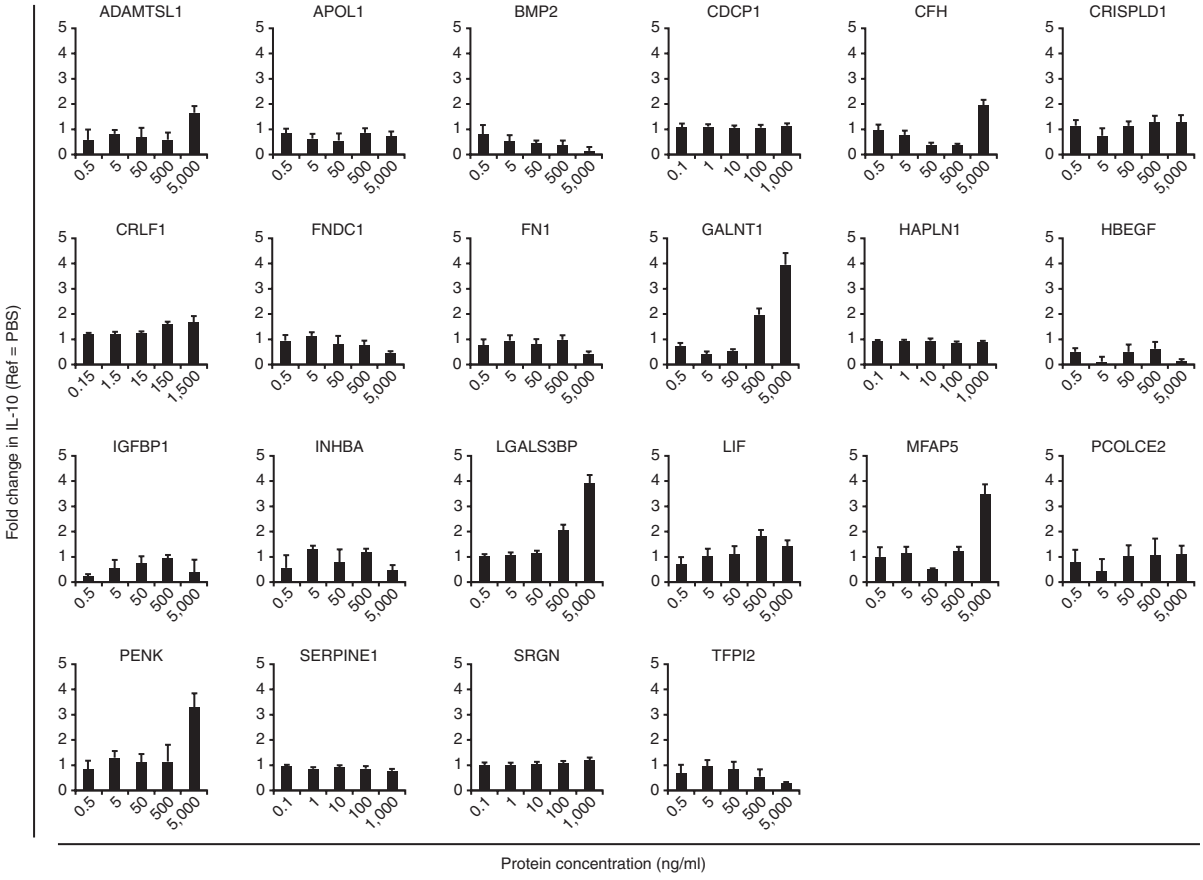

Figure 4 Screening of the enriched recombinant protein candidates. Enriched recombinant protein screen of 22 candidates using the potency assay. $N = 2$ independent trials for the entire screen, with $N > 4$ for hits.

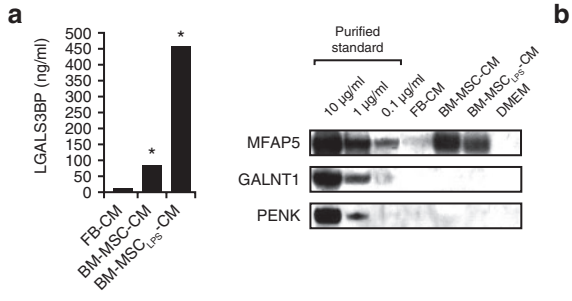

b

Protein	Identifying sequence(s)	FB	BM-MSC	BM-MSC$_{LPS}$
FN1	PAQGVVTTLENVSPPR EINLAPDSSSVVVSGLMVATK	Yes	Yes	Yes
HAPLN1	GGSDSDASLVITDLTLEDYGR LATVGELQAAWR	No	Yes	No
LGALS3BP	IYTSPTWSAFVTDSSWSAR TLQALEFHTVPFQLLAR	Yes	Yes	Yes
PCOLCE2	YDALEVFAGSGTSGQR GESGYVASEGFPNLYPPNK	Yes	No	No
SERPINE1	QFQADFTSLSDQEPLHVAQALQK VFQQVAQASK	No	No	Yes
SRGN	NLPSDSQDLGQHGLEEDFM*L GPMFELLPGESNK	No	Yes	Yes

c

Probe ID	Gene	LogFC BM-MSC-FB	P value BM-MSC-FB	LogFC BM-MSC$_{LPS}$-BM-MSC	P value BM-MSC$_{LPS}$-BM-MSC
204748_at	COX-2	-0.819365136	0.034028095	1.704844594	0.000198832
201105_at	Gal-1	-0.270354715	0.47143256	0.053125775	0.916679526
209960_at	HGF	1.618898494	0.061692046	0.524132033	0.598620893
211530_x_at	HLA-G	-0.413700228	0.055005393	0.862773913	0.002078641
210029_at	IDO	-0.081592777	0.71585143	1.97802569	0.009814786
207433_at	IL-10	-0.107545139	0.576957519	0.039924452	0.768364214
212657_s_at	IL-1RAG	0.750861416	0.018317904	3.088452263	0.000531992
205207_at	IL-6	-0.384111988	0.10494784	2.256458428	2.58E-06
210037_s_at	iNOS	-0.108988118	0.563958164	0.095508242	0.525018065
210367_s_at	PTGES	1.737782547	0.015361344	0.733193649	0.216248789
223122_s_at	SFRP2	0.112434171	0.577381131	-0.119806527	0.486219263
207643_s_at	sTNFR1	-0.233496022	0.120481789	0.319819113	0.075144505
203508_at	sTNFR2	1.136356998	0.001604751	1.224731198	0.001095973
203085_s_at	TGF- β1	0.030651866	0.911965021	0.507009083	0.232522976
209909_s_at	TGF- β2	2.537838331	0.001351263	-0.775070072	0.160136855
209747_at	TGF- β3	0.085156434	0.774108851	-0.607040448	0.078505668
206025_s_at	TSG-6	0.506390756	0.084731354	2.299118722	0.001177587

Figure 5 Assessment of BM-MSC secretion of the candidate proteins and gene expression evaluation of known therapeutic molecules produced by BM-MSCs. (**a**) ELISA and western blotting of FB-CM, BM-MSC-CM, and BM-MSC$_{LPS}$-CM for LGALS3BP, MFAP5, GALNT1, and PENK. *P < 0.001 compared to FB-CM. (**b**) Partial list of proteins contained in 150× FB-CM, BM-MSC-CM, and BM-MSC$_{LPS}$-CM detected by proteomic mass spectrometry. (**c**) Contrast gene expression data for known therapeutic molecules expressed by BM-MSCs. $N = 2$ independent batches of BM-MSCs. BM-MSC, bone marrow mesenchymal stromal cell; FB, normal human dermal fibroblasts; GALNT1, polypeptide N-acetylgalactosaminyltransferase 1; LPS, lipopolysaccharide; LGALS3BP, soluble galectin-3 binding protein; MFAP5, microfibrillar-associated protein 5; PENK, proenkephalin.

Histological analysis was also performed of liver and kidney as other prototypical organs affected by endotoxic shock, but no pathological changes were observed in any of the treatment or control arms (data not shown). The four proteins were also tested in mice challenged with a lethal dose of LPS with survival as an endpoint). Compared to anti-TNF-α antibodies, a gold-standard anti-inflammatory drug for human use,[22] MFAP5 and PENK exhibited similar protection and provided a significant survival benefit (**Figure 6c**).

CD14$^+$ human blood monocytes are the target of MFAP-5 and PENK

A target cell tracing study was conducted to better understand the underlying mechanism of action of MFAP5 and PENK. MFAP5-GST and PENK-GST were incubated separately with PBMCs prior to staining the cells with antibodies against GST and cell surface markers to delineate cell subsets. Flow cytometry revealed the CD14$^+$ fraction stained strongly for anti-GST in the presence of either of the GST-tagged proteins (**Figure 7a**). Isolated CD14$^+$ cells from whole PBMCs were then tested in our potency assay and produced the same level of IL-10 as the whole PBMC fraction when exposed to MFAP5 or PENK (**Figure 7b**), indicating that CD14$^+$ monocytes are critical mediators of the IL-10 boosting capability of MFAP5 and PENK.

DISCUSSION

EPS has several advantages over traditional methods for secreted protein discovery, making it a powerful new strategy for uncovering new pathways. First, EPS does not require LC/MS facilities but instead leverages genomic technologies that have standardized operating protocols and are now widely accessible to the biomedical research community. EPS was designed to integrate these genomic tools in a modular manner, so that new advances in tool development (*e.g.*, RNA sequencing) can also be adapted to improve EPS methods for the next generation. Second, EPS was capable of superior protein candidate detection compared to traditional LC/MS approaches that failed to reveal 86% of the proteins in the EPS-generated screening library. Third, the enrichment of candidates by EPS led to an *in vitro* hit rate of 18% and *in vivo* hit rate of 9% from a tractable library of 22 recombinant proteins. These hit rates are several orders of magnitude higher than traditional high throughput screening approaches for new chemical entities that range from 0.03 to 0.2%.[20,21] Finally, by using a phenomenological output (*i.e.*, IL-10 upregulation), this approach enabled screening without any hypotheses as to the nature or existence of receptor targets, thereby bypassing years of research required to uncover intermediate ligand–receptor interactions.

It is important to discuss the known biology of the top hits from the screen, PENK and MFAP5, as neither was previously known to possess anti-inflammatory activity. The PENK gene encodes a precursor protein that is enzymatically cleaved into proenkephalin-A-derived peptides.[23] Proenkephalin-A-derived peptides have been shown to promote lymphocyte chemotaxis,[24] suppress T-cell activation when secreted by colon cancer cells,[25]

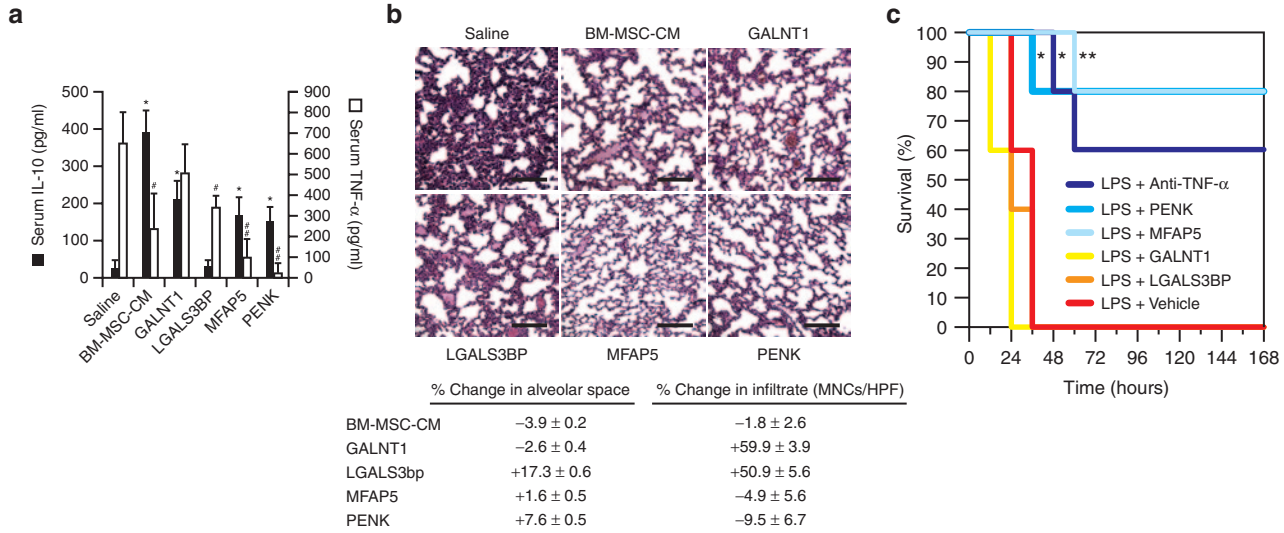

	% Change in alveolar space	% Change in infiltrate (MNCs/HPF)
BM-MSC-CM	−3.9 ± 0.2	−1.8 ± 2.6
GALNT1	−2.6 ± 0.4	+59.9 ± 3.9
LGALS3bp	+17.3 ± 0.6	+50.9 ± 5.6
MFAP5	+1.6 ± 0.5	−4.9 ± 5.6
PENK	+7.6 ± 0.5	−9.5 ± 6.7

Figure 6 *In vivo* hit screen and survival study. Proteins were administered IP at the concentration that elicited the strongest effect *in vitro*, followed by IP administration of LPS in conjunction with a second dose of the proteins 16 hours later. Two days after the combined LPS and second protein dose, the mice were sacrificed and assessed for changes in serum cytokines and tissue histology. (**a**) Serum IL-10 and serum TNF-α levels of BALB/cJ mice subjected to the *in vivo* LPS assay. **P* < 0.001 IL-10 expression compared to saline. #*P* < 0.001 TNF-α compared to saline, ##*P* < 0.05 TNF-α compared to BM-MSC-CM. *N* = 4 mice per group. (**b**) Representative micrographs of lung tissue from mice subjected to the *in vivo* LPS assay stained with hematoxylin and eosin. A table below quantifies alveolar space and mononuclear cell infiltrate per high per field in H&E sections as a % change compared to saline treated mice. A positive % change in alveolar space equates to a more normalized tissue state. A negative % change in mononuclear infiltrate would equate to normalization to a healthier tissue state. (**c**) Survival of mice subjected to a lethal dose of LPS i.p. (350 µg) concurrently with i.p. saline vehicle (bold dark blue line, *n* = 20), 300 µg/kg Anti-TNF-α antibody (thin dark blue line, *n* = 5), 200 µg/kg PENK (bold light blue line, *n* = 5) or 200 µg/kg MFAP5 (thin light blue line, *n* = 5). **P* < 0.005 compared to vehicle control, ***P* < 0.001 compared to vehicle control. Scale bar = 200 µm. i.p., intraperitoneal; LPS, lipopolysaccharide; MFAP5, microfibrillar-associated protein 5; PENK, proenkephalin; TNF, tumor necrosis factor.

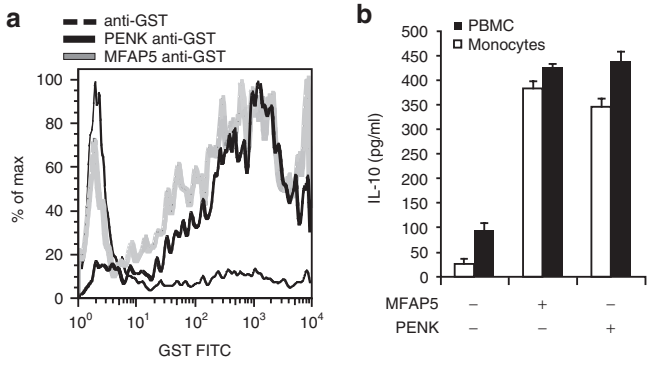

Figure 7 Identification of cellular targets of MFAP5 and PENK. (**a**) Flow cytometry of CD14⁺ cells from whole human PBMCs incubated with either MFAP5-GST, PENK-GST or no protein and then stained for GST. (**b**) LPS potency assay with PBMCs or enriched human monocytes from PBMCs and MFAP5 or PENK. BM-MSC, bone marrow mesenchymal stromal cell; FITC, fluorescein isothiocyanate; LPS, lipopolysaccharide; MFAP5, microfibrillar-associated protein 5; PBMC, peripheral blood mononuclear cells; PENK: proenkephalin.

possess antibacterial properties,[26] and, depending on the concentration, induce or suppress blastogenesis of human lymphocytes.[27] Although the downstream peptide products of PENK are responsible for observed immunomodulation, the results presented herein have discovered that the proprotein has independent immunoactivity.[24] MFAP5 is an ECM glycoprotein localized to microfibrils and associated with elastin networks. MFAP5 binds fibrillin-1 and fibrillin-2 at the C-terminus, as well as to other proteins containing EGF-like repeats.[28] Intracellular MFAP5 has been shown to interact with Notch and influence signaling, but this phenomenon has not been shown to occur with extracellular MFAP5.[29] Evidence of its relationship with the immune system is limited—to-date, there have been no accounts of MFAP5 influencing immune processes, and its connection to human inflammatory disease has not been established. It is interesting to note that the MFAP5 gene is located in the natural killer gene complex, and this location is conserved across species (observed by the authors). Perhaps, the strongest evidence that MFAP5 might play an endogenous role in immune function is seen by its relationship to cancer. It has been shown that serum MFAP5 (also known as MAGP-2) levels correlate with poor prognosis in patients with ovarian cancer.[30] In the same study, it was shown that tumor cells constitutively express MFAP5 *in vitro* and could be the source of MFAP5 secretion *in vivo*.[30] BM-MSCs are known to accumulate at malignant tumor beds and may be an additional, unidentified source of MFAP5.[31] It is conceivable, judging by their size and the pattern of secretion by BM-MSCs and other cells, that MFAP5 and derivatives of PENK are *bona fide* cytokines, and may naturally modulate other immune functions besides inflammation.[32] The EPS approach can also be positioned to uncover new biology, both in terms of understanding the endogenous role of PENK and MFAP5 by BM-MSCs and the anti-inflammatory activity these two proteins might naturally have *in vivo*.

Interestingly, neither PENK nor MFAP5 have been previously reported to be expressed by BM-MSCs nor have they been implicated in the molecular mechanisms of BM-MSC therapy.[33] In fact, the BM-MSC$_{LPS}$≥BM-MSC>FB contrast hierarchy used here highlighted a unique set of genes distinct from all previous reports of molecules critical to BM-MSC therapeutic activity (**Figure 5c**). Future studies will be needed to explore the importance of the

proteins reported here in the context of BM-MSC therapy. It is reasonable to hypothesize that the proteins that did not show IL-10 boosting activity may contribute to other anti-inflammatory responses by BM-MSCs, such as suppression of IFN-γ. Furthermore, the inability to detect levels of GALNT1 or PENK in BM-MSC CM suggests that these genes, while expressed, may not give rise to whole secreted proteins by BM-MSCs. PENK, for example, may be released as peptide derivatives of the proprotein. It is also worth noting that while these studies focused on one intersecting set of genes, the contrast hierarchy can be modified (*e.g.*, FB>BM-MSC>BM-MSC$_{LPS}$) to ask different questions about stromal cell biology and inflammation.

The results presented here suggest the native human proteins MFAP5 and PENK can attenuate inflammation by stimulating endogenous secretion of IL-10. IL-10 is a pleiotropic cytokine that downregulates Th1 cytokine expression[34] and macrophage activation[35]; increases B-cell survival, proliferation, and antibody production[36]; and is the master suppressor cytokine secreted by regulatory T cells.[37] Deficiency of IL-10 in mice results in spontaneous colitis,[38] and genetic defects in IL-10 signaling are linked to systemic lupus erythematosus,[39] Crohn's disease,[40] ulcerative colitis,[41] and Behçet's disease[42,43] in humans, suggesting an important role for the cytokine in suppressing uncontrolled inflammation in healthy individuals. IL-10 has been explored as a therapeutic in human autoimmune diseases such as psoriasis,[44] rheumatoid arthritis,[45] and Crohn's disease.[46] IL-10 has a short half-life *in vivo*, however, and trials of the recombinant protein have unfortunately failed to meet primary endpoints possibly due to limited exposure or adverse side effects when dosed at nonphysiological concentrations.[47] Boosting endogenous IL-10 with MFAP5 or PENK could overcome the limitations of exogenous IL-10 delivery by stimulating prolonged secretion of IL-10 while simultaneously allowing for natural regulatory feedback to prevent immunosuppression or severe side effects.

EPS was designed to be versatile and could be applied to other cell types for molecular discovery. The cell(s) and assay(s) can be substituted to reveal genes that are of interest to the end user. EPS may be used for freshly isolated cells thereby circumventing the requirement to grow cells *ex vivo* for LC/MS, a challenge for terminally differentiated cell types. There is also an opportunity to use different complex mixtures such as cytoplasmic or membrane fractions that are substituted in the place of a secreted mixture. With the use of different cell types, development of additional assays, and enrichment of new recombinant libraries, EPS can be a powerful discovery platform for natural protein biology and medicine.

MATERIALS AND METHODS

Statistics. Unless otherwise noted, all experiments were repeated in quadruplicate, and all data were assessed for significance using a paired, two-tailed Student's *t*-test.

Cell culture and CM. Human BM-MSCs were isolated, purified, grown, and characterized, and human skin FBs grown as described previously.[15] BM-MSCs were grown with minimum essential media—α modification (Sigma, St Louis, MO) supplemented with 10% fetal bovine serum (Atlanta Biologicals, Lawrenceville, GA), 1% antibiotic–antimycotic (Sigma), 20 mg/l gentamicin (Sigma), and 2.5 µg/l basic human fibroblastic growth factor (R&D Systems, Minneapolis, MN). Briefly, MSCs isolated from human bone marrow aspirates (Lonza, Walkersville, PA), were plated onto T175 flasks at a seeding density of 1,000 cells/cm^2. After 10 days of growth, the BMSCs were rinsed with phosphate-buffered saline (PBS) twice and incubated at 37 °C with Trypsin (Life Technologies, Grand Island, NY) for 12 minutes to dislodge the cells from the flask for subsequent passaging. Cells were cryopreserved at a concentration of 1×10^6 cells/ml in minimum essential media—α modification containing 10% fetal bovine serum, 10% dimethyl sulfoxide (Sigma), and 1% penicillin–streptomycin (Sigma). Cells were confirmed for a CD45$^-$, CD146$^+$, CD44$^+$, and CD105$^+$ phenotype using flow cytometry (**Supplementary Figure S1**). Antibodies used were: CD45-fluorescein isothiocyanate (FITC), CD44-APC, CD105-PE, CD11b-FITC, and CD146-FITC (BD Biosciences, Franklin Lakes, NJ). Data were acquired using a FACSCalibur (BD Biosciences).

BM-MSCs were used at passage 2–5, which was equivalent to 5–20 population doublings from the bank created from a bone marrow donation. The CM was also collected and concentrated as described previously.[15] Harvested CM was stored at 4 degrees for no longer than 2 weeks before concentration and use. For BM-MSC$_{LPS}$ CM and cells used for gene expression analysis, BM-MSCs were grown to >80% confluence and rinsed twice with PBS. BM-MSC expansion medium, supplemented with 1 µg/ml LPS (*Escherichia coli* 0111:B4; Sigma), was then added to the cells for 24 hours. After this stimulation period, the cells were again rinsed with PBS twice and incubated for an additional 24 hours with serum-free Dulbecco's modified Eagle medium to produce CM. In the majority of experiments, CM was concentrated by 15× using Amicon filtration columns (Millipore, Billerica, MA) with a 3kDa cut-off. This was achieved when 15 ml of conditioning medium was incubated in the presence of 2×10^6 cells for 24 hours, collected, and concentrated to a final volume of 1 ml. In certain cases, the medium was concentrated to 7.5× or 150×.

Prestimulation of BM-MSCs. BM-MSCs were cultured and expanded until >80% confluent. The culture medium was aspirated and the cells rinsed twice with PBS. Culture medium was added to the cells supplemented with varying concentrations of the following: IFN-γ (0.1 µg/l), TNF-α (0.1 µg/ml), IL-6 (1 ng/ml), and IL-1β (1 ng/ml) (R&D Systems); Poly I:C DNA (10 µg/ml) (Invivogen, San Diego, CA); and LPS (1 µg/ml) (*E. coli* 0111:B4; Sigma). The cells were incubated in the presence of these additives for 24 hours, followed by aspiration of the supernatant, two washes with PBS, and addition of Dulbecco's modified Eagle medium conditioning medium. The Dulbecco's modified Eagle medium conditioning medium was incubated in the presence of the cells for 24 hours when it was collected and concentrated as for BM-MSC-CM.

PBMC potency assay. The assay was performed as before.[15] Approval for the collection of blood from healthy volunteers was obtained from the Institutional Review Board of Massachusetts General Hospital. Human PBMCs were isolated using a ficoll gradient (density = 1.077 g/cc; GE Healthcare, Uppsala, Sweden). The buffy coat was then washed in media, centrifuged at 1,500 rpm, and resuspended for cell counting. PBMCs were seeded in 96-well round bottom plate at 50 µl per well (100,000 cells per well) and incubated at 37 °C for with BMSC-CM or proteins for 18 hours before LPS stimulation. For the majority of the experiments, the potency assay was terminated at 5 hours for IL-10 analysis.

Staining for the target cell of MFAP5 and PENK. PBMCs were collected and incubated on ice for 30 minutes in RPMI 1640 (Sigma), or in RPMI 1640 containing 1 U/ml of MFAP5-GST or PENK-GST (Abnova, Taipei, Taiwan). The cells were then spun down and washed once with PBS prior to being resuspended in RPMI containing 100 µg/ml of FITC-anti-GST antibodies (Abcam, Cambridge, MA), and incubated for 30 minutes on ice. The cells were then spun down and washed once with PBS prior to fixing with 2% PFA. The fixed cells were then analyzed using flow cytometry for FITC-positive cells. Forward- and side scattering of FITC-positive cells indicated a population overlapping with the predicted size and granularity

of monocytes, and the experiment was repeated as described above with the addition of 10 μg/ml of PERCP-anti-CD14 during the anti-GST staining step. No other populations of cells stained strongly for MFAP5 or PENK.

Purifying primary human monocytes. PBMCs were isolated from 25 ml of freshly isolated whole human blood via ficoll gradient (density = 1.077 g/cc; GE Healthcare), and then monocytes were negatively selected using a selection kit using the manufacturer's instructions (Pan Monocyte Isolation Kit; Miltenyi Biotec, Bergisch Gladbach, Germany). A small sample of enriched monocytes was stained as indicated above for CD14 to determine purity using flow cytometry, and only enrichment of >70% was considered acceptable for future experimentation. For experiments that compared purified monocytes to PBMCs in the same assay format as the PBMC potency assay, 10^5 PBMCs were used per well, and 10^4 purified monocytes. This proportion of monocytes in the PBMC fraction (10% of PBMCs) was based on flow cytometry of $CD14^+$ stained PBMCs.

Gene expression analysis. Gene expression was evaluated using Affymetrix GeneChip Human Genome U133 Plus 2.0 Arrays (Affymetrix, Santa Clara, CA). Array quality was assessed using the R/Bioconductor package.[48] All arrays passed visual inspection and no technical outliers were identified ($n = 3$ arrays per cell type). Raw CEL files were processed using the robust multiarray average algorithm.[49] To identify genes correlating with the observed phenotypic groups, we used limma[50] to fit a statistical linear model to the data and then tested for differential gene expression in the contrasts of interest: FB versus BM-MSC; BM-MSC versus LPS. Results were adjusted for multiple testing using the Benjamini and Hochberg method,[51] and significance was determined using a false-discovery-rate cutoff of less than 1%. All genes identified to be upregulated in BM-MSCs compared to FBs and either expressed equally or upregulated in BM-MSC_{LPS} compared to BM-MSCs were then analyzed by literature review for definitive evidence of production of a secreted protein by human cells to generate the list of genes reported here. Independent analysis conducted in collaboration with a second computational biology facility confirmed these same results with >95% overlap of secreted proteins identified via literature review.

Recombinant protein screen. Recombinant proteins were acquired from a commercial vendor (Abnova). Quality control tests were performed on each lot of new protein to confirm and normalize potency for each batch. The amount of protein needed to induce a twofold increase in IL-10 was considered as a unit of drug material and showed an approximate range of ± 50% difference in protein mass between batches. The proteins were diluted in PBS and added to the PBMC potency assay to achieve a range of final concentrations spanning ~1 μg/ml to ~0.01 ng/ml.

ELISAs and western blots. The ELISA kits used were provided by commercial vendors and were used according to the manufacturers' instructions (IL-10 in cell supernatants: BD Biosciences; LGALS3BP: Abnova; IL-10 and TNF-α from animal serum: R&D Systems). To blot for GALNT1, MFAP5 and PENK, FB-CM, BM-MSC-CM, and BM-MSC_{LPS}-CM were run out using protein gel electrophoresis (Pierce, Rockford, IL) followed by blotting using detection antibodies (Sigma) applied at a dilution of 1:500 (GALNT1 and MFAP5) or 1:100 (PENK), and corresponding secondary antibodies (anti-rabbit for GALNT1 and MFAP5 and anti-goat for PENK) conjugated with HRP (Sigma). For the LGALS3BP ELISA and the MFAP5 blot, 1× conditioned media were used, and for the GALNT1 and PENK blots, 1-100× conditioned media were used.

MS. MS was performed at the MS core facility of the Beth Israel Deaconess Medical Center at Harvard Medical School as previously described.[52] 10× samples of BM-MSC-CM, FB-CM, and BM-MSC_{LPS}-CM were initially separated by sodium dodecyl sulfate–polyacrylamide gel electrophoresis and bands were excised and trypsin digested for analysis via tandem LC/MS/MS. The false discovery rate for peptide identifications was ~ 1.5% and less than 0.5% for protein identifications.

In vivo *mouse assay.* All procedures were performed in accordance with the animal rights policies of the Massachusetts General Hospital Subcommittee on Research Animal Care. For the sublethal LPS model, 8-week-old female BALB/cJ mice ($n \geq 3$) (Jackson Laboratories, Bar Harbor, ME) were administered an initial dose of either vehicle or one of the experimental therapies IP: 200 μl of saline (vehicle), or 3 μg of protein (*e.g.*, GALNT1, LGALS3BP, MFAP5, or PENK) diluted in 200 μl of saline, or 1 ml of 15× BM-MSC-CM. Sixteen hours later, the mice received a second dose of either vehicle or therapy in conjunction with a dose of 100 μg of LPS (*E. coli* 0111:B4; Sigma) diluted in physiological saline. Fourty-eight hours later, the mice were sacrificed and tissue and blood were collected for analysis. The serum was tested for the presence of IL-10 and TNF-α via ELISA and the lungs, livers, and kidneys of the animals were preserved for hematoxylin and eosin staining. For the lethal LPS model, 8-week-old female BALB/cJ mice ($n \geq 5$) were coadministered a lethal dose of LPS (350 μg LPS in 100 μl physiological saline) and either vehicle (negative control), 5 μg anti-TNF-α (positive control; R&D Systems), 4 μg MFAP5 diluted in 100 μl of physiological saline, or 4 μg of PENK diluted in 100 μl of physiological saline. The mice were monitored for survival for 7 days (168 hours).

Quantification of lung histology. Quantification of mononuclear cells and alveolar space in H&E stained lung sections was performed in 10 random per animal using the public software ImageJ (http://rsb.info.nih.gov/ij/). Mononuclear cells were quantified using particle counts of nuclei that were set with appropriate criteria for a specific threshold of staining intensity as well as corresponding sizes of the nuclei. Nuclei of area less than 500 $pixel^2$ were analyzed to identify infiltrating inflammatory cells from lung parenchyma and resident nonparenchymal cells. Alveolar space was calculated using a threshold function of ImageJ, excluding edges of images, which calculated the area of only multicellular structures enclosing central whitespace at ×10 magnification. Data are presented as percentage differences of each parameter compared to saline-treated LPS mice as a baseline.

SUPPLEMENTARY MATERIAL

Figure S1. Flow cytometry of BM-MSCs.
Figure S2. IL-10 assay time course and effect of proteinase K on the activity of BM-MSC-CM.
Figure S3. Interferon-γ potency assay.
Figure S4. Liquid chromatography of BM-MSC-CM.
Materials and Methods

ACKNOWLEDGMENTS

We would like to acknowledge John Asara for assistance with the mass spectrometry, Mick Correll for assistance with the gene expression analysis, and Patricia Della Pelle and Ryan Murray for assistance with histology and image acquisition. We would also like to acknowledge David Yarmush and Michael Cima for helpful discussions and insight. The research was funded in part by grants from the National Institutes of Health: K01DK087770 (B.P.), R01EB012521 (B.P.), R01DK43371 (M.L.Y.), the Shriners Hospitals for Children (B.P.). J.M.M. was partially supported by a training grant from the National Human Genome Research Institute (T32 HG002295). J.M.M. conceived the ideas, designed and executed the experiments, interpreted data, and wrote the manuscript. M.L. designed and executed the experiments. A.G. analyzed the gene expression data. M.F. performed the western blots. Y.J. assisted in the recombinant protein screen. J.L. assisted in the animal experiments. M.L.Y. interpreted data and provided funding. B.P. conceived the ideas, designed and executed the experiments, interpreted data, wrote the manuscript, and provided funding. J.M.M., M.L., M.L.Y., and B.P. are listed as inventors on a patent application that pertains to the presented results.

REFERENCES

1. Nakamura, T, Nishizawa, T, Hagiya, M, Seki, T, Shimonishi, M, Sugimura, A *et al.* (1989). Molecular cloning and expression of human hepatocyte growth factor. *Nature* **342**: 440–443.
2. Heinzel, FP, Sadick, MD, Holaday, BJ, Coffman, RL and Locksley, RM (1989). Reciprocal expression of interferon gamma or interleukin 4 during the resolution or progression

of murine leishmaniasis. Evidence for expansion of distinct helper T cell subsets. *J Exp Med* **169**: 59–72.
3. Leung, DW, Cachianes, G, Kuang, WJ, Goeddel, DV and Ferrara, N (1989). Vascular endothelial growth factor is a secreted angiogenic mitogen. *Science* **246**: 1306–1309.
4. Suda, T, Takahashi, T, Golstein, P and Nagata, S (1993). Molecular cloning and expression of the Fas ligand, a novel member of the tumor necrosis factor family. *Cell* **75**: 1169–1178.
5. Daneman, D (2006). Type 1 diabetes. *Lancet* **367**: 847–858.
6. Aggarwal, SR (2012). What's fueling the biotech engine-2011 to 2012. *Nat Biotechnol* **30**: 1191–1197.
7. Manns, MP, McHutchison, JG, Gordon, SC, Rustgi, VK, Shiffman, M, Reindollar, R *et al.* (2001). Peginterferon alfa-2b plus ribavirin compared with interferon alfa-2b plus ribavirin for initial treatment of chronic hepatitis C: a randomised trial. *Lancet* **358**: 958–965.
8. Taylor, PC and Feldmann, M (2009). Anti-TNF biologic agents: still the therapy of choice for rheumatoid arthritis. *Nat Rev Rheumatol* **5**: 578–582.
9. Guzman, C, and Feuerstein, G (eds) (2009). Pharmaceutical Biotechnology. Landes Bioscience and Springer Science+Business Media: Austin, Texas, USA.
10. Harrison, PM, Kumar, A, Lang, N, Snyder, M and Gerstein, M (2002). A question of size: the eukaryotic proteome and the problems in defining it. *Nucleic Acids Res* **30**: 1083–1090.
11. Rubinstein, M, Rubinstein, S, Familletti, PC, Gross, MS, Miller, RS, Waldman, AA *et al.* (1978). Human leukocyte interferon purified to homogeneity. *Science* **202**: 1289–1290.
12. Montesano, R, Matsumoto, K, Nakamura, T and Orci, L (1991). Identification of a fibroblast-derived epithelial morphogen as hepatocyte growth factor. *Cell* **67**: 901–908.
13. Elias, JE and Gygi, SP (2007). Target-decoy search strategy for increased confidence in large-scale protein identifications by mass spectrometry. *Nat Methods* **4**: 207–214.
14. Sharma, K, Weber, C, Bairlein, M, Greff, Z, Kéri, G, Cox, J *et al.* (2009). Proteomics strategy for quantitative protein interaction profiling in cell extracts. *Nat Methods* **6**: 741–744.
15. Jiao, Y, Milwid, JM, Yarmush, ML, and Parekkadan, B (2010). A Mesenchymal Stem Cell Potency Assay. In: Cuturi, M and Anegon, I (eds). *Suppression and Regulation of Immune Responses*, vol. 677. Humana Press and Springer: Totowa, New Jersey, USA.
16. Parekkadan, B and Milwid, JM (2010). Mesenchymal stem cells as therapeutics. *Annu Rev Biomed Eng* **12**: 87–117.
17. Uccelli, A, Moretta, L and Pistoia, V (2008). Mesenchymal stem cells in health and disease. *Nat Rev Immunol* **8**: 726–736.
18. van Poll, D, Parekkadan, B, Cho, CH, Berthiaume, F, Nahmias, Y, Tilles, AW *et al.* (2008). Mesenchymal stem cell-derived molecules directly modulate hepatocellular death and regeneration *in vitro* and in vivo. *Hepatology* **47**: 1634–1643.
19. Tomchuck, SL, Zwezdaryk, KJ, Coffelt, SB, Waterman, RS, Danka, ES and Scandurro, AB (2008). Toll-like receptors on human mesenchymal stem cells drive their migration and immunomodulating responses. *Stem Cells* **26**: 99–107.
20. Kwok, TC, Ricker, N, Fraser, R, Chan, AW, Burns, A, Stanley, EF *et al.* (2006). A small-molecule screen in C. elegans yields a new calcium channel antagonist. *Nature* **441**: 91–95.
21. Hung, DT, Shakhnovich, EA, Pierson, E and Mekalanos, JJ (2005). Small-molecule inhibitor of Vibrio cholerae virulence and intestinal colonization. *Science* **310**: 670–674.
22. Sheridan, C (2008). Small molecule challenges dominance of TNF-alpha inhibitors. *Nat Biotechnol* **26**: 143–144.
23. Gubler, U, Seeburg, P, Hoffman, BJ, Gage, LP and Udenfriend, S (1982). Molecular cloning establishes proenkephalin as precursor of enkephalin-containing peptides. *Nature* **295**: 206–208.
24. Heagy, W, Laurance, M, Cohen, E and Finberg, R (1990). Neurohormones regulate T cell function. *J Exp Med* **171**: 1625–1633.
25. Ohmori, H, Fujii, K, Sasahira, T, Luo, Y, Isobe, M, Tatsumoto, N *et al.* (2009). Methionine-enkephalin secreted by human colorectal cancer cells suppresses T lymphocytes. *Cancer Sci* **100**: 497–502.
26. Goumon, Y, Lugardon, K, Kieffer, B, Lefèvre, JF, Van Dorsselaer, A, Aunis, D *et al.* (1998). Characterization of antibacterial COOH-terminal proenkephalin-A-derived peptides (PEAP) in infectious fluids. Importance of enkelytin, the antibacterial PEAP209-237 secreted by stimulated chromaffin cells. *J Biol Chem* **273**: 29847–29856.
27. Roscetti, G, Ausiello, CM, Palma, C, Gulla, P and Roda, LG (1988). Enkephalin activity on antigen-induced proliferation of human peripheral blood mononucleate cells. *Int J Immunopharmacol* **10**: 819–823.
28. Penner, AS, Rock, MJ, Kielty, CM and Shipley, JM (2002). Microfibril-associated glycoprotein-2 interacts with fibrillin-1 and fibrillin-2 suggesting a role for MAGP-2 in elastic fiber assembly. *J Biol Chem* **277**: 35044–35049.
29. Miyamoto, A, Lau, R, Hein, PW, Shipley, JM and Weinmaster, G (2006). Microfibrillar proteins MAGP-1 and MAGP-2 induce Notch1 extracellular domain dissociation and receptor activation. *J Biol Chem* **281**: 10089–10097.
30. Mok, SC, Bonome, T, Vathipadiekal, V, Bell, A, Johnson, ME, Wong, KK *et al.* (2009). A gene signature predictive for outcome in advanced ovarian cancer identifies a survival factor: microfibril-associated glycoprotein 2. *Cancer Cell* **16**: 521–532.
31. Lazennec, G and Jorgensen, C (2008). Concise review: adult multipotent stromal cells and cancer: risk or benefit? *Stem Cells* **26**: 1387–1394.
32. Hook, S, Camberis, M, Prout, M, Konig, M, Zimmer, A, Van Heeke, G *et al.* (1999). Preproenkephalin is a Th2 cytokine but is not required for Th2 differentiation *in vitro*. *Immunol Cell Biol* **77**: 385–390.
33. Pittenger, M (2009). Sleuthing the source of regeneration by MSCs. *Cell Stem Cell* **5**: 8–10.
34. de Waal Malefyt, R, Abrams, J, Bennett, B, Figdor, CG and de Vries, JE (1991). Interleukin 10(IL-10) inhibits cytokine synthesis by human monocytes: an autoregulatory role of IL-10 produced by monocytes. *J Exp Med* **174**: 1209–1220.
35. Bogdan, C, Vodovotz, Y and Nathan, C (1991). Macrophage deactivation by interleukin 10. *J Exp Med* **174**: 1549–1555.
36. Rousset, F, Garcia, E, Defrance, T, Péronne, C, Vezzio, N, Hsu, DH *et al.* (1992). Interleukin 10 is a potent growth and differentiation factor for activated human B lymphocytes. *Proc Natl Acad Sci U S A* **89**: 1890–1893.
37. Asseman, C, Mauze, S, Leach, MW, Coffman, RL and Powrie, F (1999). An essential role for interleukin 10 in the function of regulatory T cells that inhibit intestinal inflammation. *J Exp Med* **190**: 995–1004.
38. Kühn, R, Löhler, J, Rennick, D, Rajewsky, K and Müller, W (1993). Interleukin-10-deficient mice develop chronic enterocolitis. *Cell* **75**: 263–274.
39. Gateva, V, Sandling, JK, Hom, G, Taylor, KE, Chung, SA, Sun, X *et al.* (2009). A large-scale replication study identifies TNIP1, PRDM1, JAZF1, UHRF1BP1 and IL10 as risk loci for systemic lupus erythematosus. *Nat Genet* **41**: 1228–1233.
40. Noguchi, E, Homma, Y, Kang, X, Netea, MG and Ma, X (2009). A Crohn's disease-associated NOD2 mutation suppresses transcription of human IL10 by inhibiting activity of the nuclear ribonucleoprotein hnRNP-A1. *Nat Immunol* **10**: 471–479.
41. Franke, A, Balschun, T, Karlsen, TH, Sventoraityte, J, Nikolaus, S, Mayr, G *et al.*; IBSEN study group. (2008). Sequence variants in IL10, ARPC2 and multiple other loci contribute to ulcerative colitis susceptibility. *Nat Genet* **40**: 1319–1323.
42. Mizuki, N, Meguro, A, Ota, M, Ohno, S, Shiota, T, Kawagoe, T *et al.* (2010). Genome-wide association studies identify IL23R-IL12RB2 and IL10 as Behçet's disease susceptibility loci. *Nat Genet* **42**: 703–706.
43. Remmers, EF, Cosan, F, Kirino, Y, Ombrello, MJ, Abaci, N, Satorius, C *et al.* (2010). Genome-wide association study identifies variants in the MHC class I, IL10, and IL23R-IL12RB2 regions associated with Behçet's disease. *Nat Genet* **42**: 698–702.
44. Asadullah, K, Sterry, W, Stephanek, K, Jasulaitis, D, Leupold, M, Audring, H *et al.* (1998). IL-10 is a key cytokine in psoriasis. Proof of principle by IL-10 therapy: a new therapeutic approach. *J Clin Invest* **101**: 783–794.
45. Keystone, E, Wherry, J and Grint, P (1998). IL-10 as a therapeutic strategy in the treatment of rheumatoid arthritis. *Rheum Dis Clin North Am* **24**: 629–639.
46. Li, MC and He, SH (2004). IL-10 and its related cytokines for treatment of inflammatory bowel disease. *World J Gastroenterol* **10**: 620–625.
47. Mosser, DM and Zhang, X (2008). Interleukin-10: new perspectives on an old cytokine. *Immunol Rev* **226**: 205–218.
48. Gentleman, RC, Carey, VJ, Bates, DM, Bolstad, B, Dettling, M, Dudoit, S *et al.* (2004). Bioconductor: open software development for computational biology and bioinformatics. *Genome Biol* **5**: R80.
49. Irizarry, RA, Bolstad, BM, Collin, F, Cope, LM, Hobbs, B and Speed, TP (2003). Summaries of Affymetrix GeneChip probe level data. *Nucleic Acids Res* **31**: e15.
50. Smyth, GK (2004). Linear models and empirical bayes methods for assessing differential expression in microarray experiments. *Stat Appl Genet Mol Biol* **3**: Article3.
51. Benjamini, Y, and Hochberg, Y (1995). Controlling the false discovery rate: a practical and powerful approach to multiple testing. *J Royal Statistical Society Series B (Methodological)* **57**: 289–300.
52. Jiang, X, Chen, S, Asara, JM and Balk, SP (2010). Phosphoinositide 3-kinase pathway activation in phosphate and tensin homolog (PTEN)-deficient prostate cancer cells is independent of receptor tyrosine kinases and mediated by the p110beta and p110delta catalytic subunits. *J Biol Chem* **285**: 14980–14989.